Trying to Understand the Interstellar Transport and Resulting Anisotropies of Galactic Cosmic

J. R. Jokipii
University of Arizona

Presented at the Madison Cosmic-Ray Anisotropy Workshop

Outline

- Background/Introduction
- Transport Approximations
- Anisotropies
  - Small-Scale
    - Heliospheric Tail?
    - Effects of Interstellar Turbulence?
  - Large-Scale
    - Observed Lifetimes and Anisotropies
    - Effects of interstellar turbulence?

The observed quiet-time cosmic-ray spectrum

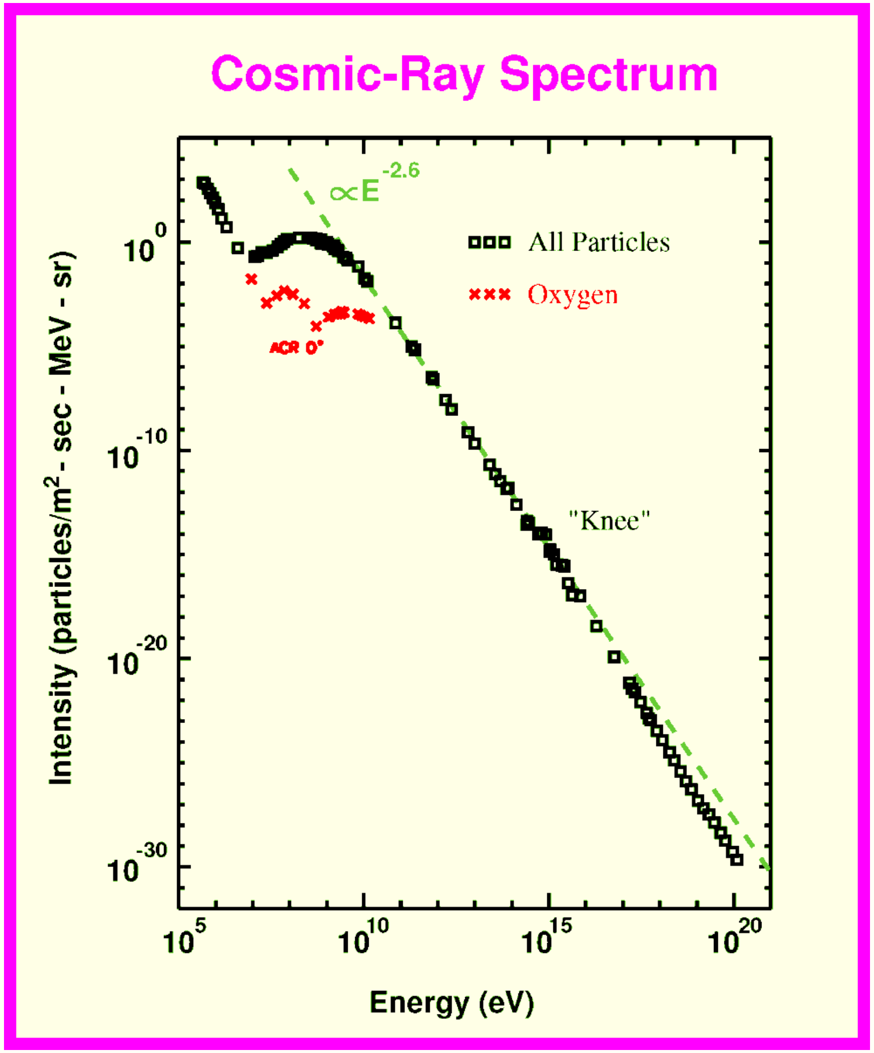

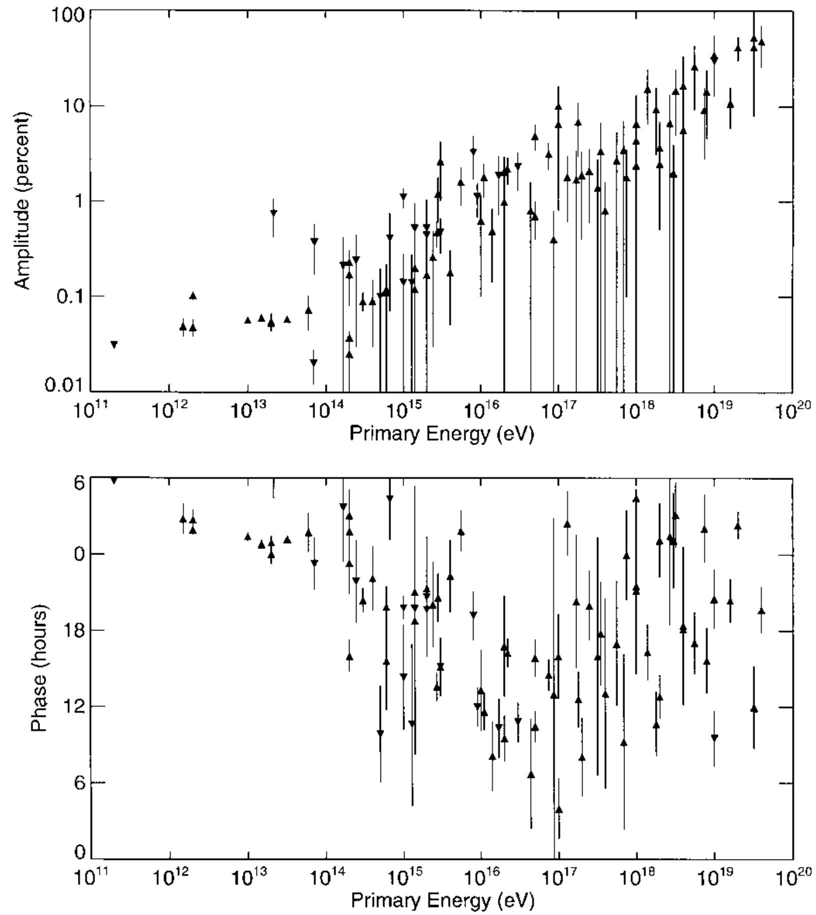

Fig. 7. A compilation of anisotropy measurements (first harmonic Fourier amplitude and phase). Northern and southern hemisphere results are denoted by upward-pointing and downward-pointing triangles, respectively. (From Clay and Smith [76].)

First, consider the small-scale anisotropies.

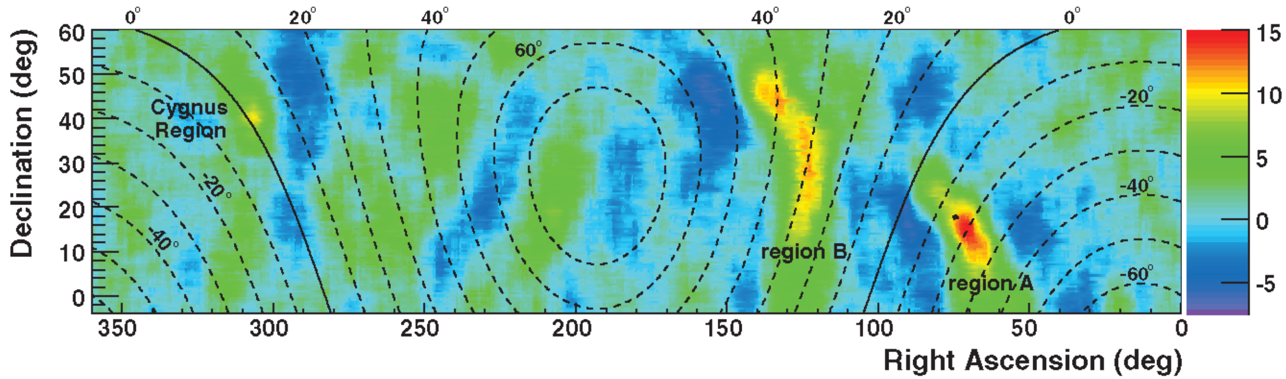

FIG. 1 (color). Map of significances for the Milagro data set without any cuts to remove the hadronic cosmic-ray background. A 10° bin was used to smooth the data, and the color scale gives the significance. The solid line marks the Galactic plane, and every 10° in

the
ion
the

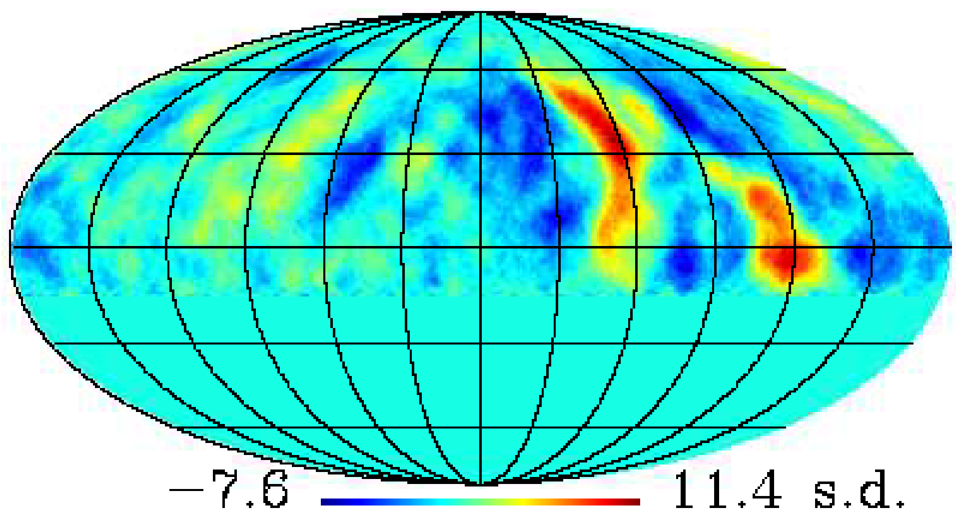

Fig. 1: Sky map in equatorial coordinates obtained in 424 days of measurements, for events with $N_{pad} \geq 40$. The right ascension is equal to zero on the extreme right of the map and increases going towards the left. The color scale indicates the statistical significance in standard deviations.

Heliospheric Cause?

- Lazarian and Desiati suggested that the excess from the direction of the heliotail was caused by particle acceleration in reconnection events in magnetic structures in the tail.

- They did not present a detailed mechanism for the acceleration, but stated that the gyro-radii of the relevant particles could be contained in the tail. ?

- The acceleration must come from the ambient electric field E = U x B/c.

Question: Can the Heliosphere accelerate ~ several TeV particles to produce the anisotropies?

- The acceleration must come from the electric field E ~ (U/c) B
- $U \sim V_a \sim 100$ km/sec
- $B \sim 10^{-6}$ G
- $\Delta T \sim q E L$
- $Q = 4.8 \times 10^{-10}$, L~100 AU
- $\Rightarrow \Delta T \sim 100$ MeV
- $\Rightarrow$ Anisotropy ~ few times $\Delta T/T \sim 3\text{x}10^{-5}$
- This is just close enough to 10^{-4} to be possible.

Another question: could the observed enhancements be caused by simple motions in the heliotail magnetic field?

Or, could the enhancement in the heliotail direction be a coincidence?

Consider another possibility: Could the enhancement be a consequence of particle motions in the turbulent interstellar magnetic field?

A slightly related idea was discussed by Malkov etal, 2010.

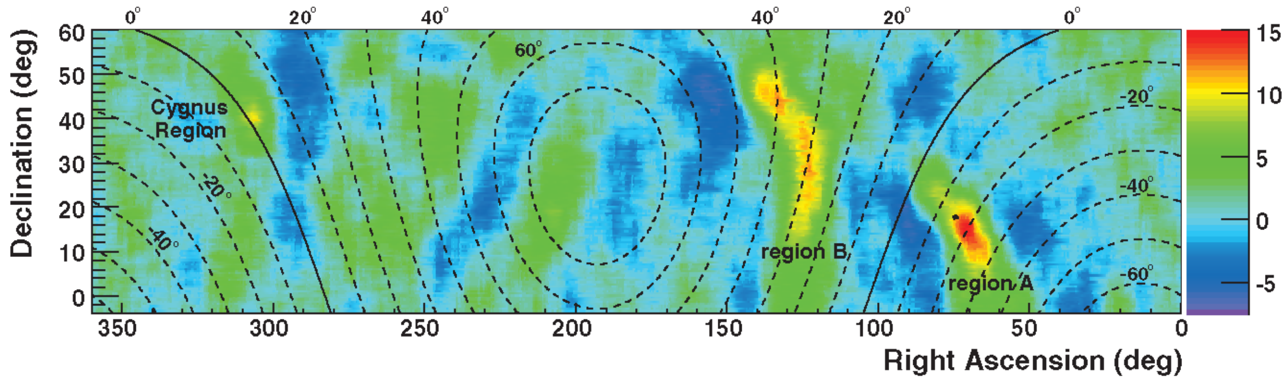

FIG. 1 (color). Map of significances for the Milagro data set without any cuts to remove the hadronic cosmic-ray background. A 10° bin was used to smooth the data, and the color scale gives the significance. The solid line marks the Galactic plane, and every 10° in

the

ion

the

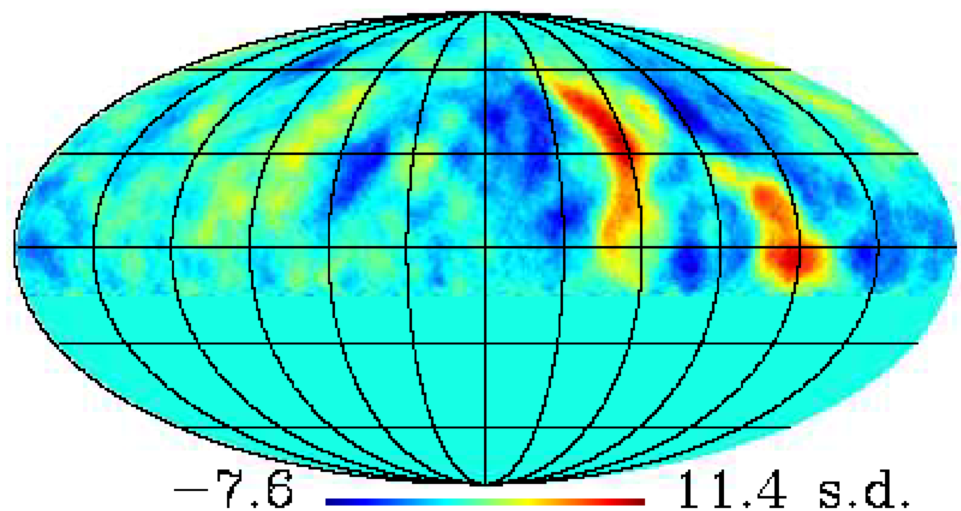

Fig. 1: Sky map in equatorial coordinates obtained in 424 days of measurements, for events with $N_{pad} \geq 40$. The right ascension is equal to zero on the extreme right of the map and increases going towards the left. The color scale indicates the statistical significance in standard deviations.

Another Possibility

- The small-scale anisotropies could be unrelated to CR sources, or the heliotail, but instead could CR intensity fluctuations be caused by the turbulent magnetic-field.
- This is indeed observed in the inner heliosphere, and is termed ‘interplanetary cosmic-ray scintillations’. See Owens and Jokipii, 1973, 1974.
- The fluctuating magnetic field causes fluctuations in the cosmic rays – $n = n_0 + n_1$.
- If n_1 is small, o lowest order in n_1 / n_0 one finds, after a Fourier transform:

$$[\, i(\omega - k \cdot w) - \omega_o \, \partial / \partial \phi] \; n_1 (k, w, \omega) = - \epsilon_{ijk} \; w_i \, \omega_{1k}(k, \omega) \{\partial n_0 / \partial w_i \}$$

Comparison of the observed temporal power spectrum of neutron-monitor scintillations with theory, using the observed interplanetary magnetic-field power spectrum.

In the ISM we should compare the anisotropy angular variation spectrum with theory using the interstellar power spectrum.

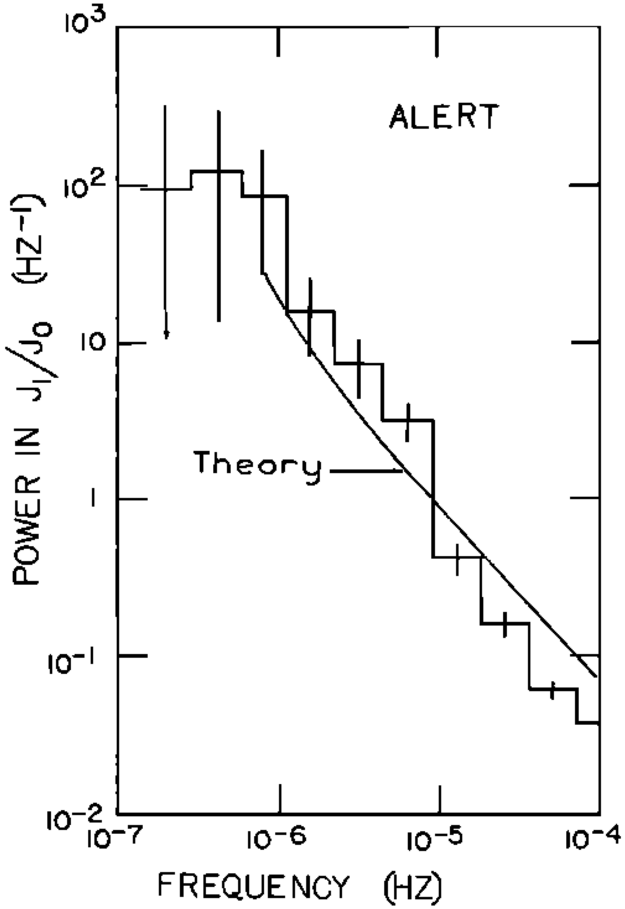

Fig. 3. Power spectrum of the flux of the Alert neutron monitor. The histograms give the observed power spectrum for a 90-day quiet period in 1969 along with 90% confidence intervals. The Poisson noise level $P_p(f) = 2/I$ for the spectrum is $\sim 10^{-2}$ Hz^{-1}. The curve is the result of the theory (equation 15) when the model shown in Figure 1 is used.

Motion in an irregular magnetic field is chaotic:
This demonstrates the importance of small-scale turbulence.

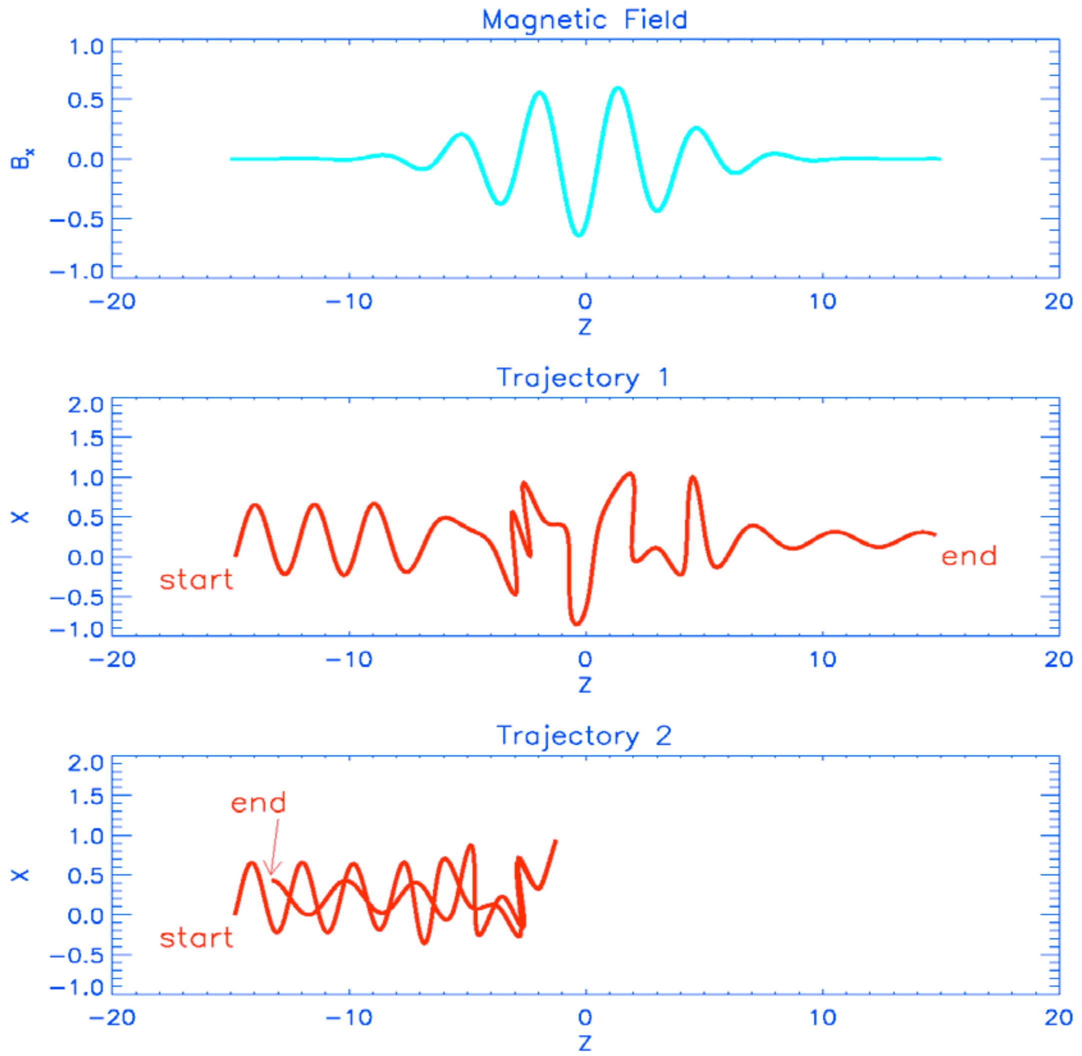

The observed spectrum of interstellar-medium fluctuations

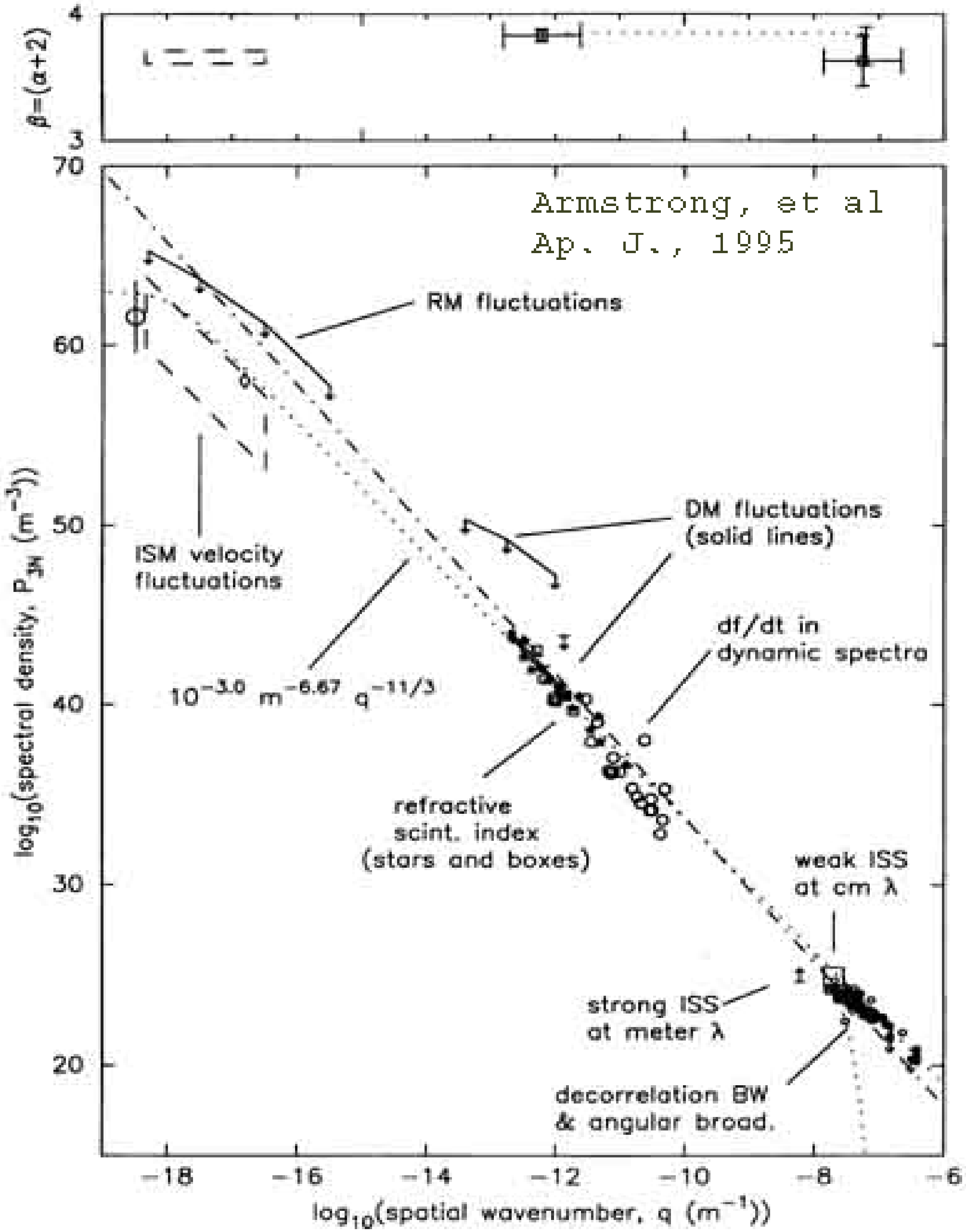

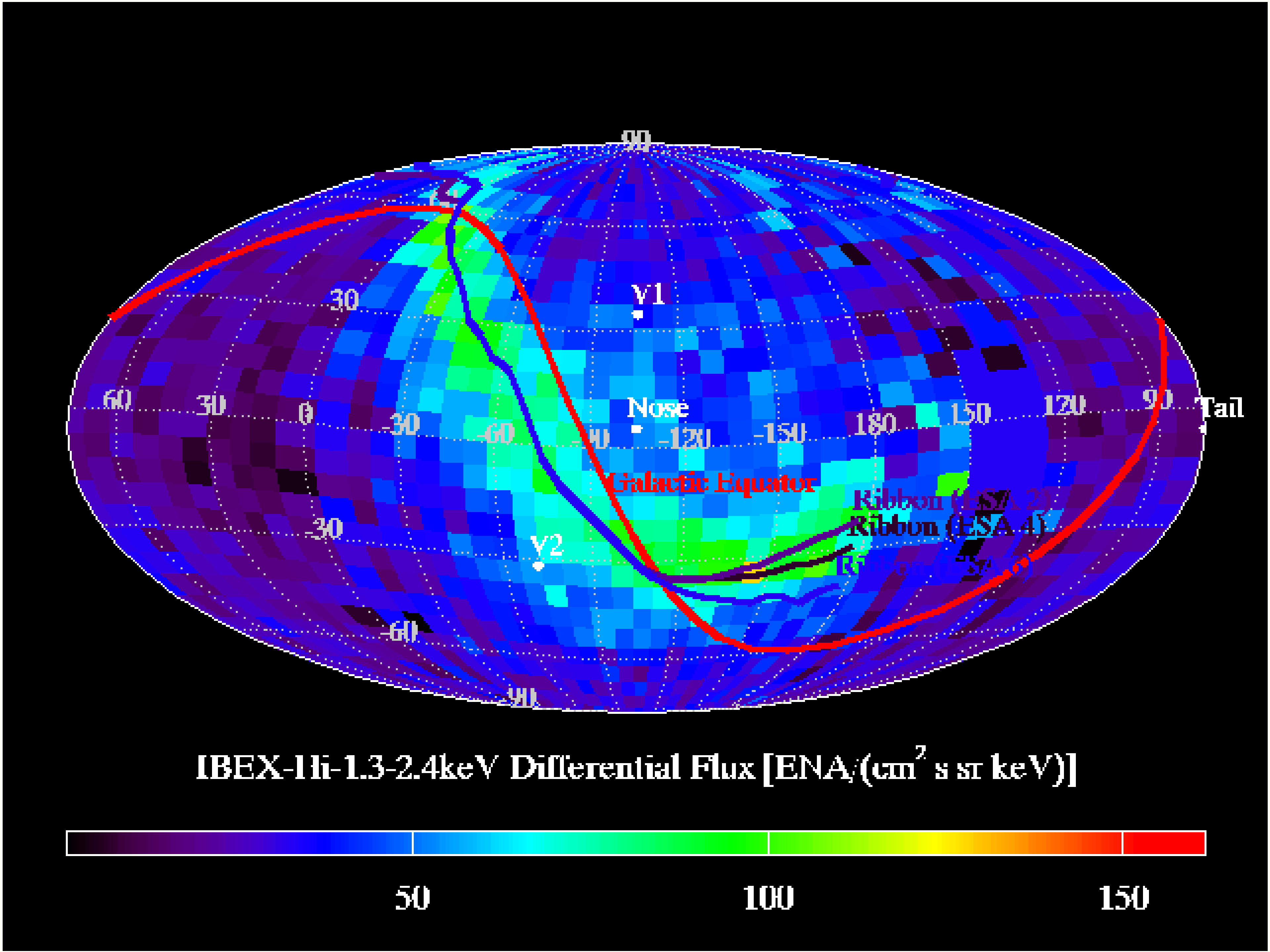

V1
Nose
Tail
V2
Galactic Equator
Ribbon (ESA 2)
Ribbon (ESA 4)
IBEX-Hi-1.3-2.4keV Differential Flux [ENA/(cm2 s sr keV)]
50
100
150

The interstellar magnetic field is nearly constant on the relevant ~several-hundred AU s

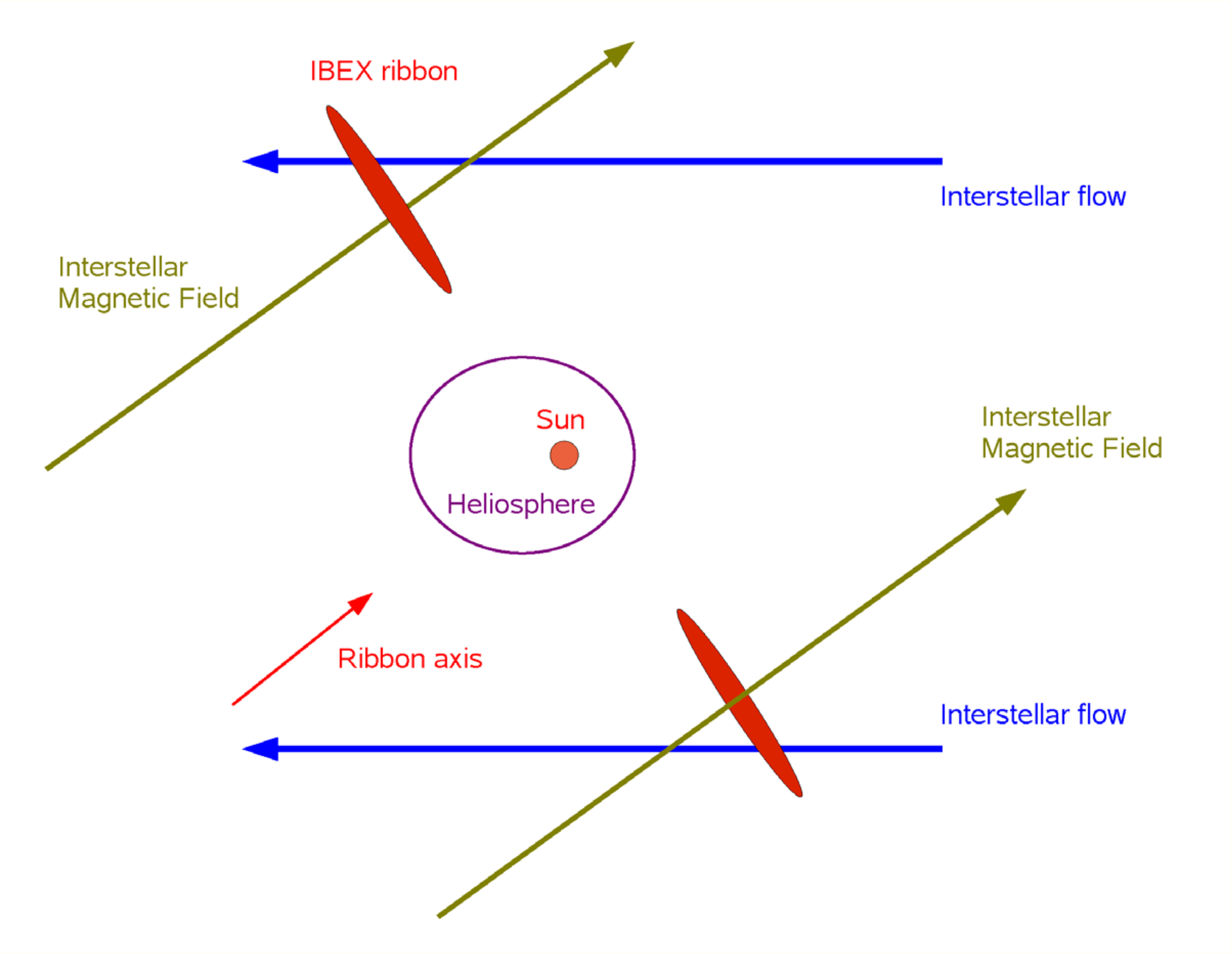

The effect of the turbulence on the ribbon can be illustrated in this cartoon.

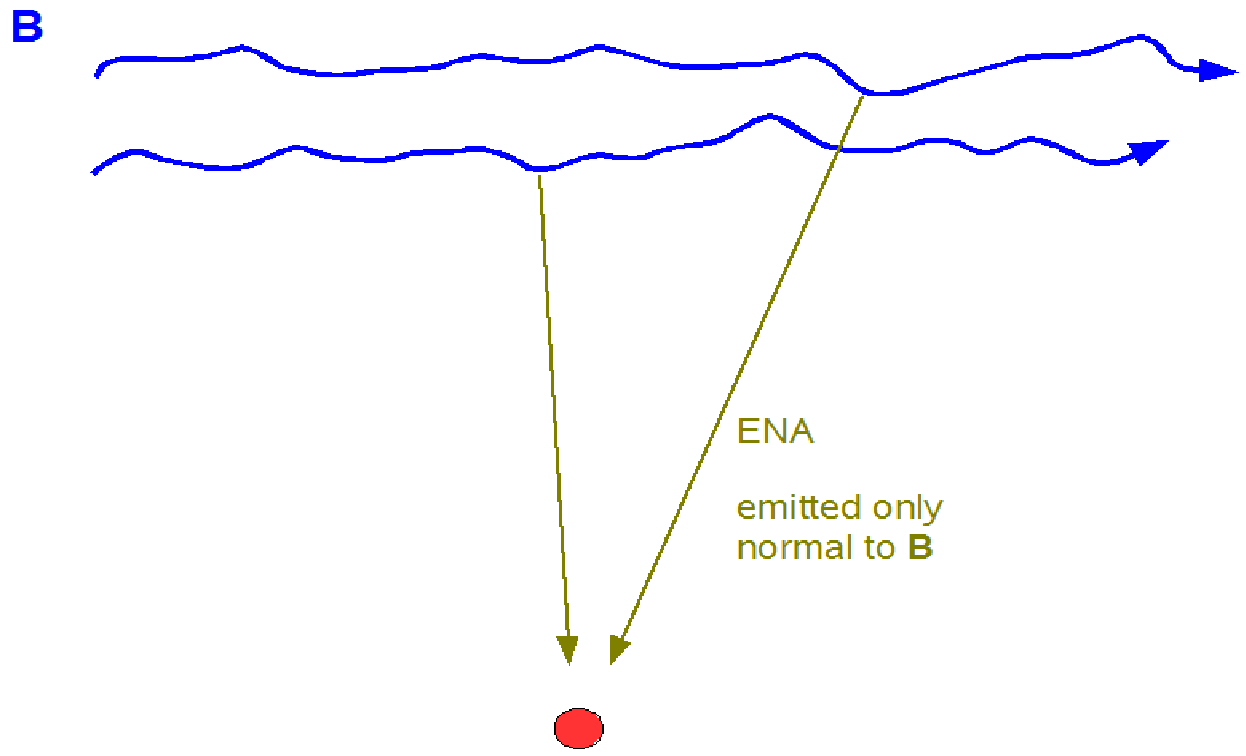

The magnetic-field fluctuations above are exaggerated to illustrate the point. Clearly the fluctuations in the magnetic field will broaden the emissions in the direction along the average magnetic field.

The Puzzle of the Large-Scale (first harmonic) Anisotropy

- This anisotropy is generally associated with the escape of the bulk of the cosmic rays from the galaxy, presumably by a diffusive process.

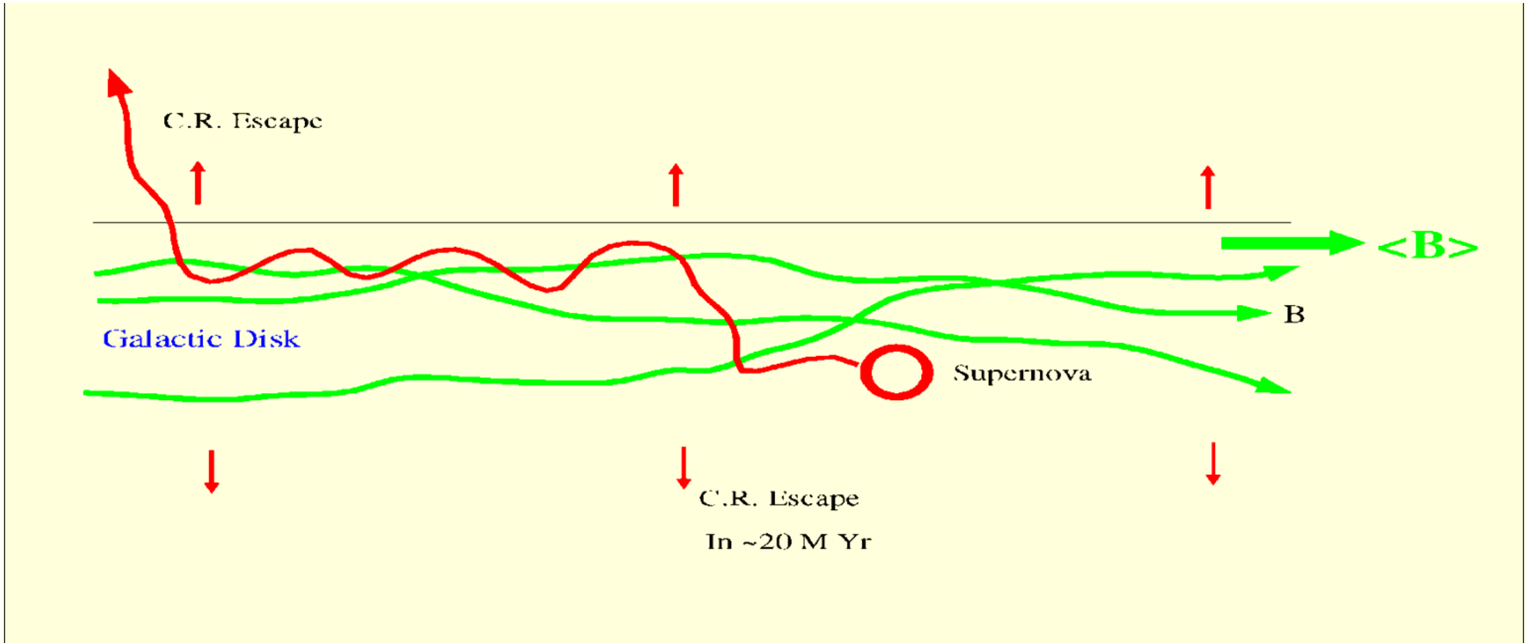

Use the Parker Transport Equation:

$$\frac{\partial f}{\partial t} = \frac{\partial}{\partial x_i}\left[\kappa_{ij}^{(S)} \frac{\partial f}{\partial x_j}\right]$$ $\Rightarrow$ **Diffusion**

$$-\mathbf{U} \cdot \nabla f$$ $\Rightarrow$ **Convection w. plasma**

$$-\mathbf{V_d} \cdot \nabla f$$ $\Rightarrow$ **Grad & Curvature Drift**

$$+\tfrac{1}{3}\nabla \cdot \mathbf{U}\left[\frac{\partial f}{\partial \ell np}\right]$$ $\Rightarrow$ **Energy change – electric field**

$$+Q$$ $\Rightarrow$ **Source**

Where the drift velocity due to the large scale curvature and gradient of the average magnetic field is:

$$\mathbf{V_d} = \frac{pcw}{3q} \nabla \times \left[\frac{\mathbf{B}}{B^2}\right] = \nabla \cdot \kappa_{\mathbf{A}}$$

The associated anisotropy is obtained from the diffusive streaming flux

$S_i = -\kappa_{ij} \partial f / \partial x_i + (U_i/3) p \partial f /\partial p$

or bulk velocity S_i/w, which then gives the anisotropy

$\delta_i = 3 S_i/w$

here w is the particle speed.

If U is small, one can generally estimate the anisotropy as $\delta \approx \lambda /L$, where λ is the mean free path and L is the macroscopic scale.

The turbulent electromagnetic field is described statistically. In the quasilinear approximation, the scattering rate $\nu \propto P_B[1/(r_c \cos \theta_{p)})]$. Notice also the large-scale field-line meandering.

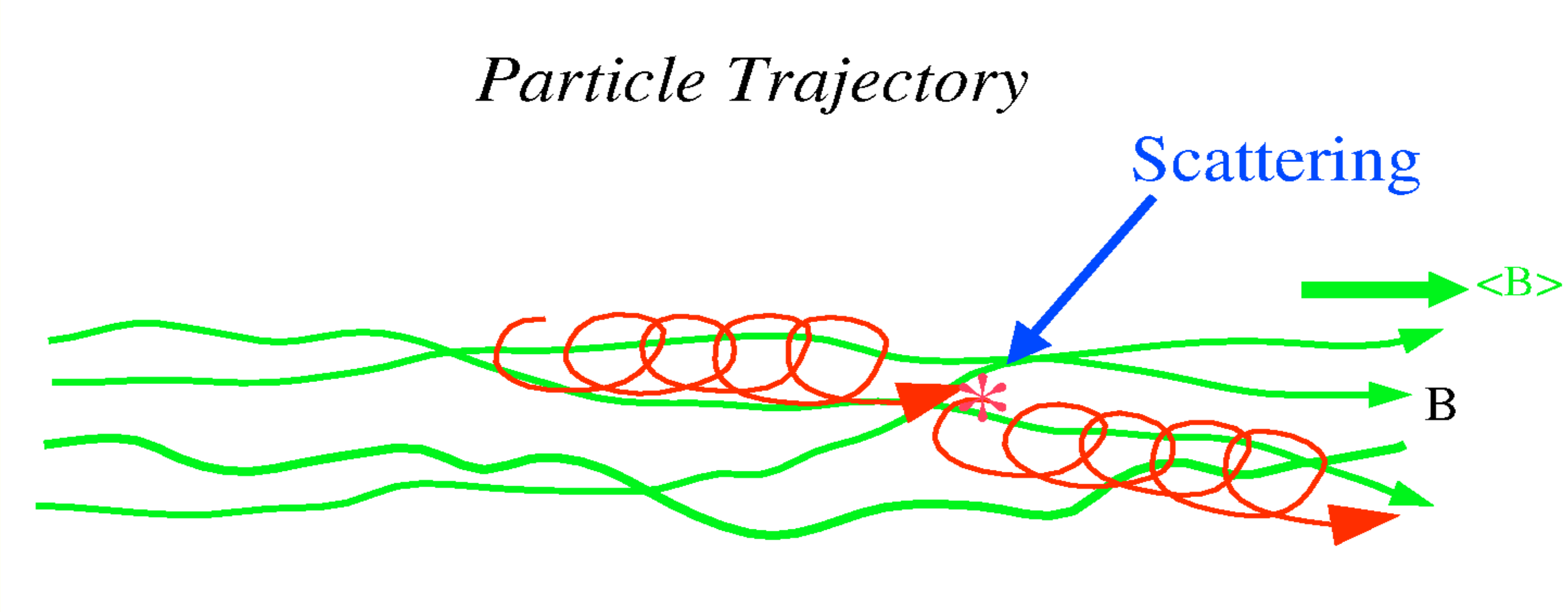

Test-Particle Simulations using synthesized Kolmogorov turbulence (Gicalone and Jokipii, Ap. J. 1999 + 1 point)

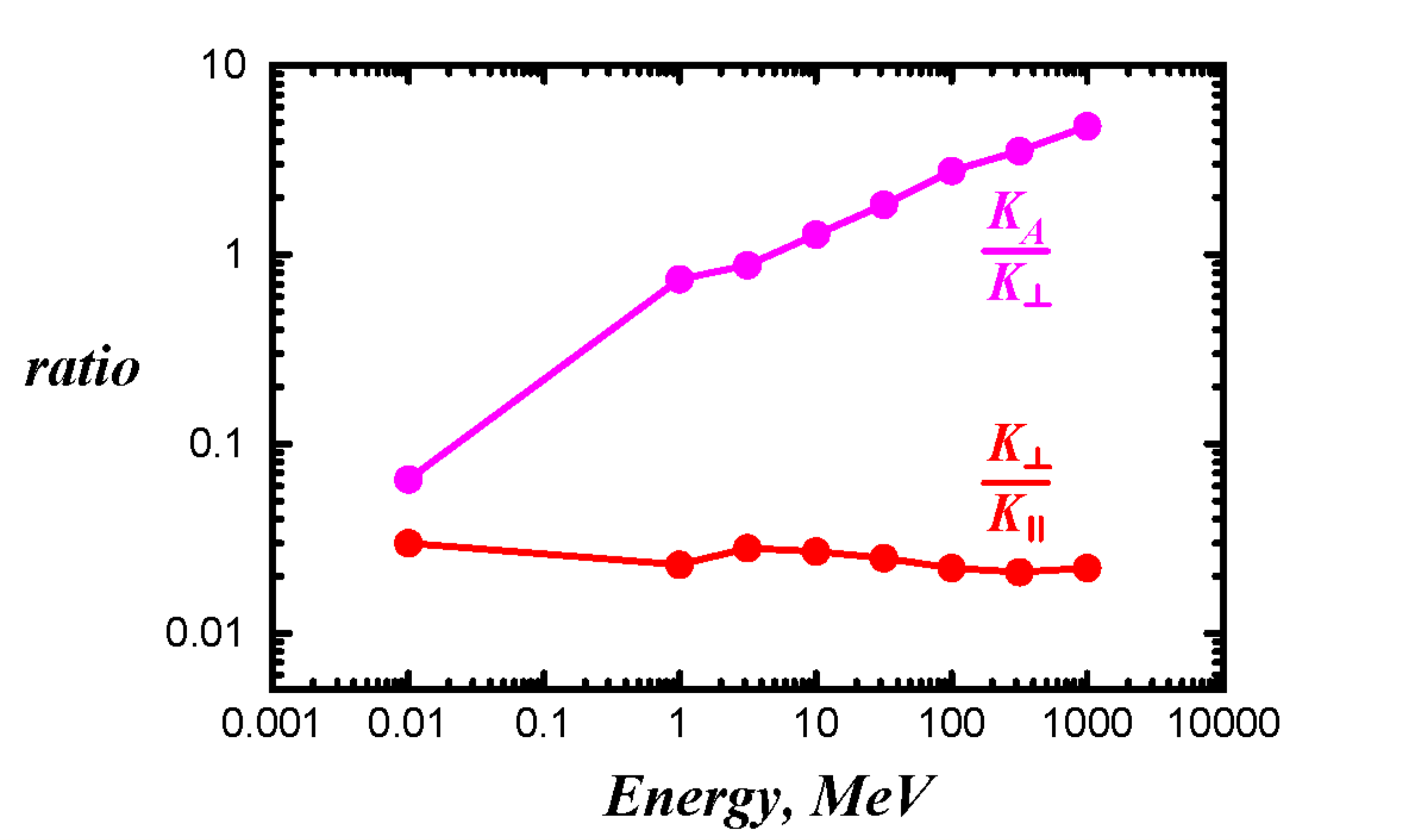

We *never* find the classical condition $\kappa_\perp = \kappa_\parallel / (1+\omega^2 \tau^2)$ which would give a *much* smaller ratio.

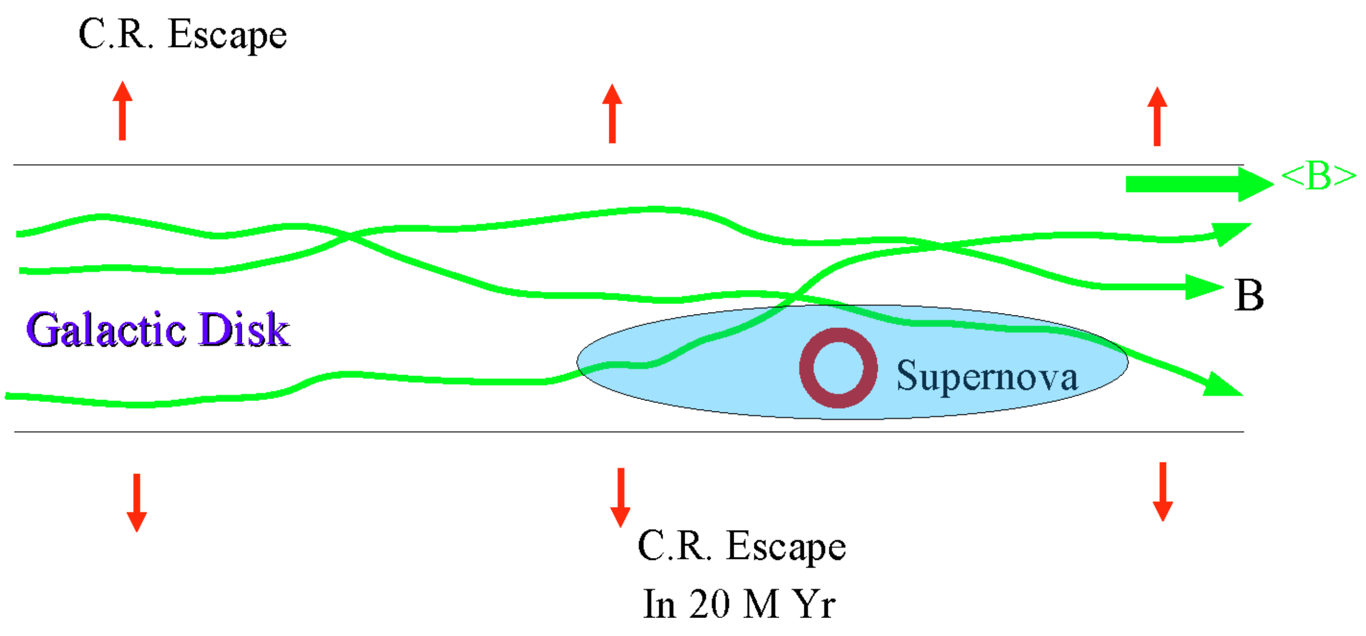
C.R. Escape
<B>
B
Galactic Disk
Supernova
C.R. Escape
In 20 M Yr

Transport and Loss in the Galaxy

The transport equation is sometimes simplified to the very simple and basic equation

$$\partial f / \partial t \approx 0 \approx - f / \tau_L + Q$$

or

$$f = \tau_L \; Q$$

where f is the distribution function ($dj/dT = p^2 f$, where p is the momentum of the particle), $\tau \approx L^2 / \kappa_\perp$ and Q is the source of particles. For relativistic particles pc = T. Primary cosmic rays are accelerated from ambient material, presumably at supernova blast waves In this case Q_p is a power law: $Q_p(T) \propto T^{-(2-2.3)}$

The characteristic loss time τ_L can be determined from secondary nuclei, produced from collisions (spallation) with ambient gas.

Since, at high energies, the spallation approximately conserves energy per nucleon, we have the source of secondaries $Q_s \propto f_p$

Then we have

$f_s = \tau_L Q_s \propto \tau_L f_p$ or $f_s/f_p \propto \tau_L$

This ratio is observed to vary as $\approx T^{-0.6}$ at $T \approx$ 1-10 GeV.

Extrapolated to high Energies, this gives problems.

Observations show that $\tau_L \approx$ 20 Myr at GeV energies, or some 300 yr at 10^{18} eV!

We may inquire as to how large the perpendicular diffusion coefficient must be to yield .

$\tau_L \approx L^2/\kappa_\perp$ to be $\approx 2 \times 10^7$ yrs

Setting L equal to a characteristic scale normal to the disk of some 500 pc yields $\kappa_\perp \approx 4 \times 10^{27}$ cm^2/sec, which is quite large.

A typically quoted value for $\kappa_{\|}$ of the order of or less than 10^{29} cm^2/sec, in which case the ratio of perpendicular to parallel diffusion is about 4%.

These considerations seem reasonable.

Associated Anisotropy

- Strictly speaking we should not do anisotropies in the leaky box model.
- Nonetheless, simple considerations lead to reasonable anisotropies at GeV energies.
- In the diffusion approximation (the Parker equation), we can write for the anisotropy

$c\,\delta \approx 3(L/\tau_L)$

or

$\delta \approx 3\,L/(\tau_L\,c) \approx \text{few} \times 10^{-4}$ relative to the local plasma, which is not unreasonable.

BUT, what happens at high energies?

- We must remember that observations mandate that τ_L scale as $T^{0.6}$, at least at ~ several GeV energies.

- This would give $\delta \approx 1$ at 10^{18} eV !!

- Observations give $\delta < \approx 5\%$.

- The theoretical scaling of τ_L as $T^{.33}$ for Kolmogorov turbulence is barely acceptable at about 5%. But this would change the τ_L

From Bhattachargee and Sigl (2000)

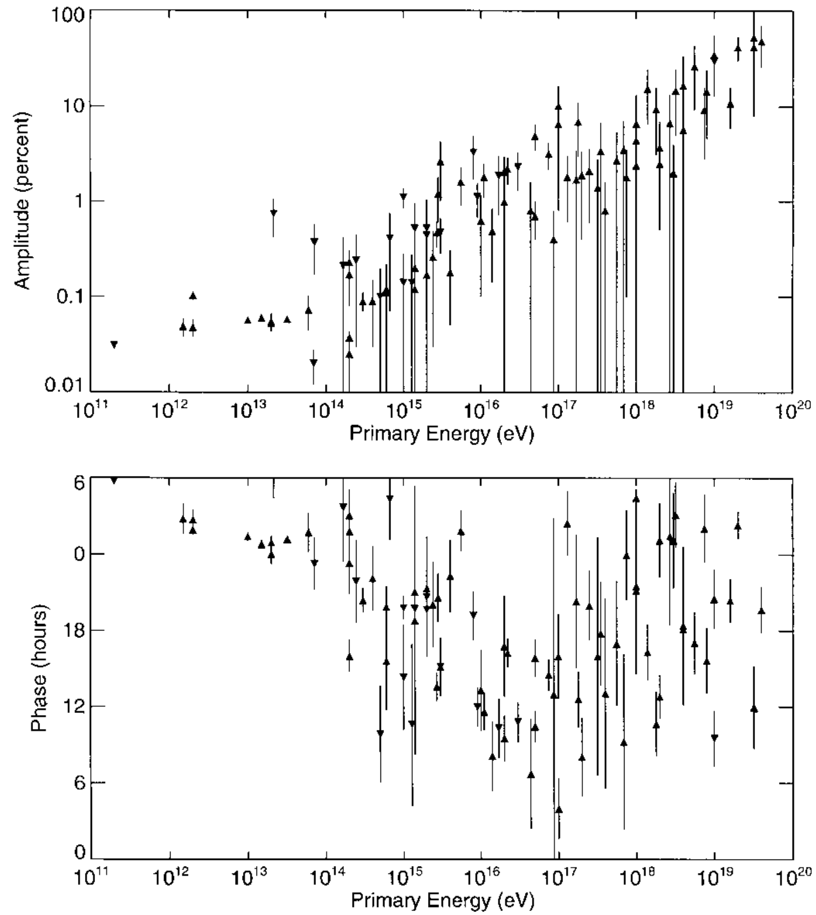

Fig. 7. A compilation of anisotropy measurements (first harmonic Fourier amplitude and phase). Northern and southern hemisphere results are denoted by upward-pointing and downward-pointing triangles, respectively. (From Clay and Smith [76].)

What is the alternative?

- The above arguments are quite basic.
- Perhaps the answer is to consider more-realistic geometries.
- We are observing near the center of the galactic disk. In this case, the gradients and hence the anisotropies can be much smaller.

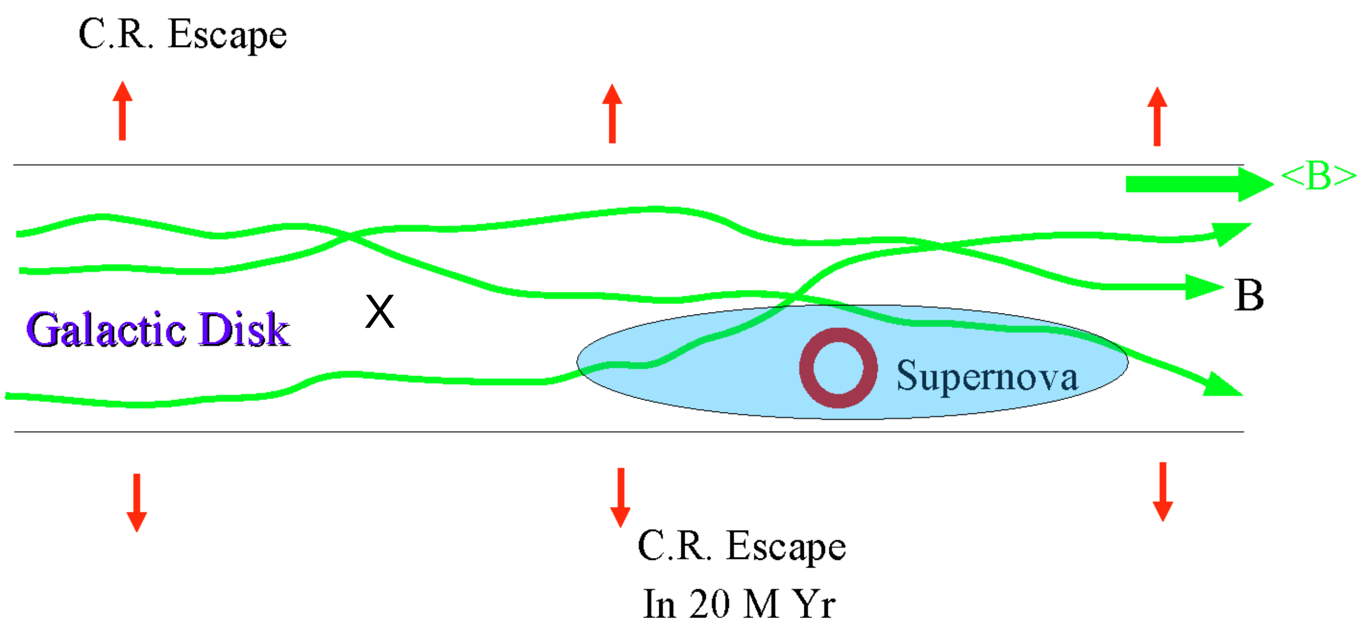
C.R. Escape
<B>
B
Galactic Disk
X
Supernova
C.R. Escape
In 20 M Yr

Results of a simple 1-dimensional model which illustrates the point

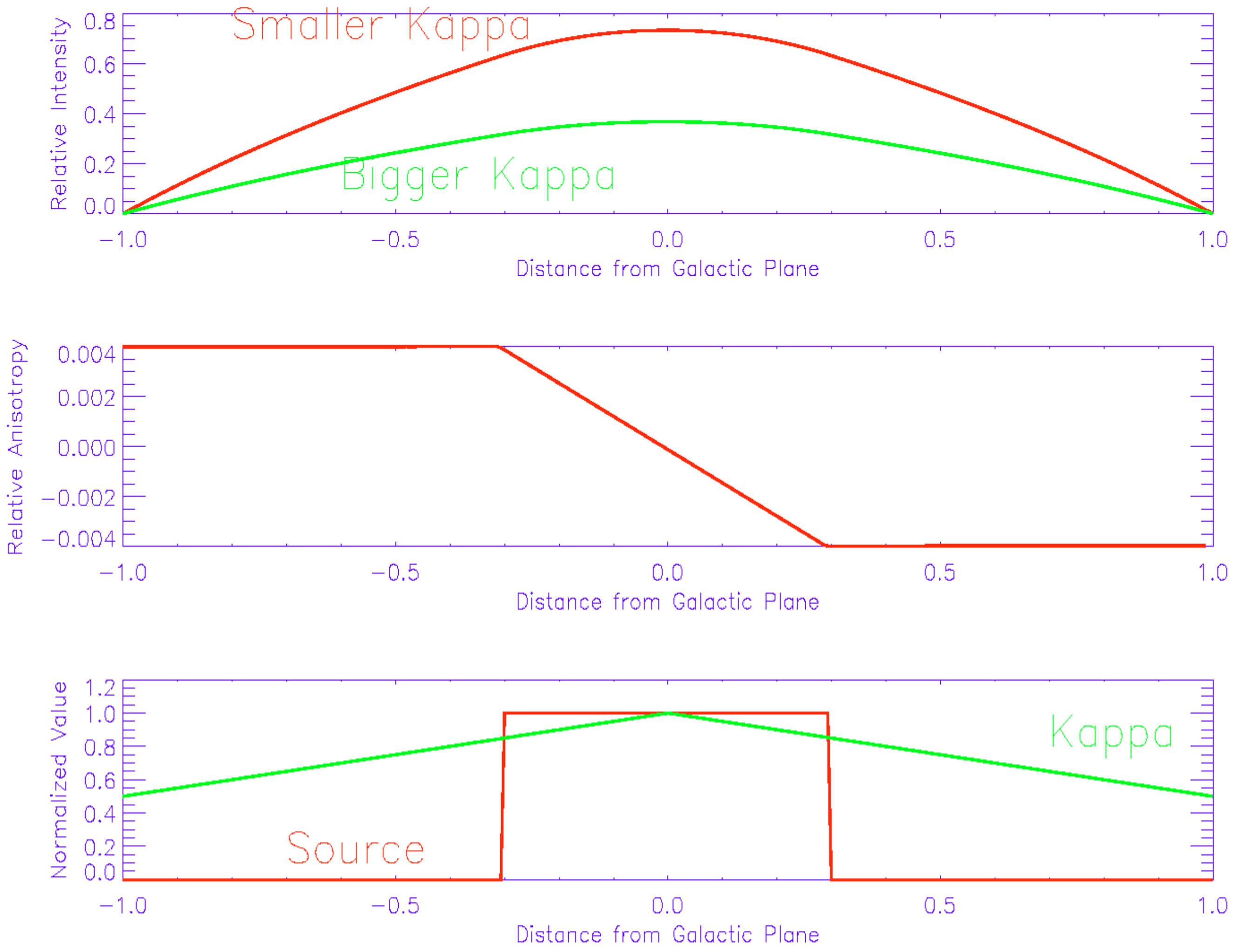

Large-scale interstellar fluctuations or turbulence will also play a significant role.

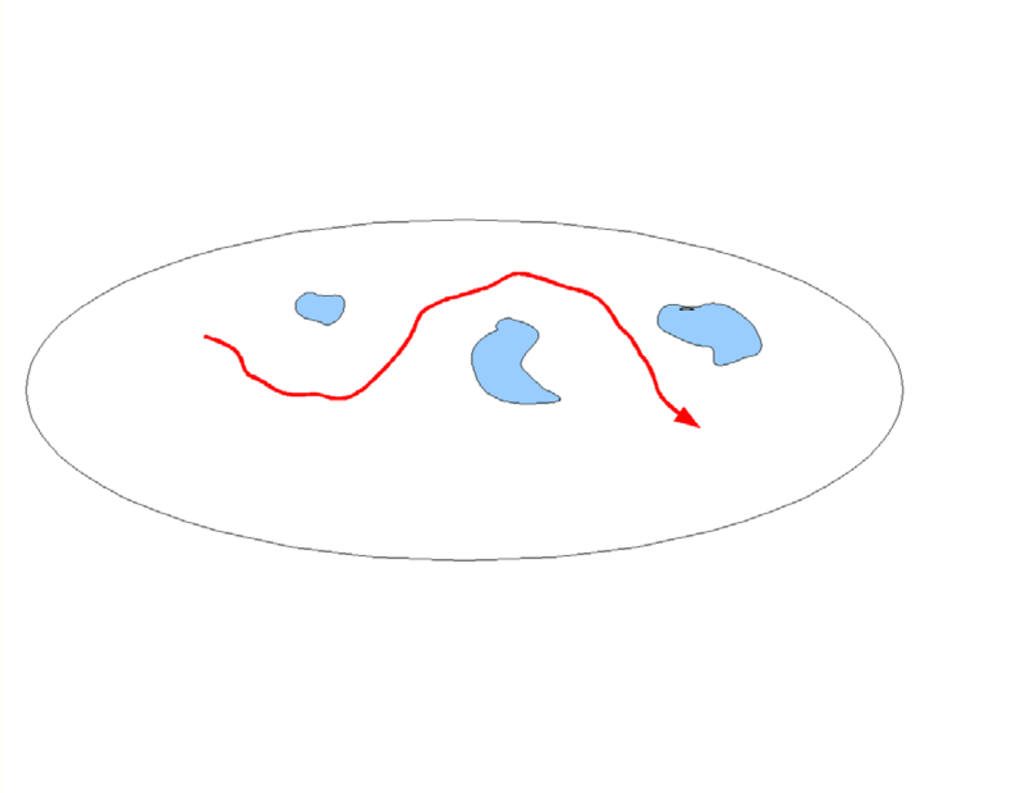

A simple, illustrative, model.

The results of a stochastic 2-D integration of Parker's transport equation for a fluctuating diffusion coefficient.

The source is at the center and the outer escape boundary is a circle.

Note: a one-D model is not interesting.

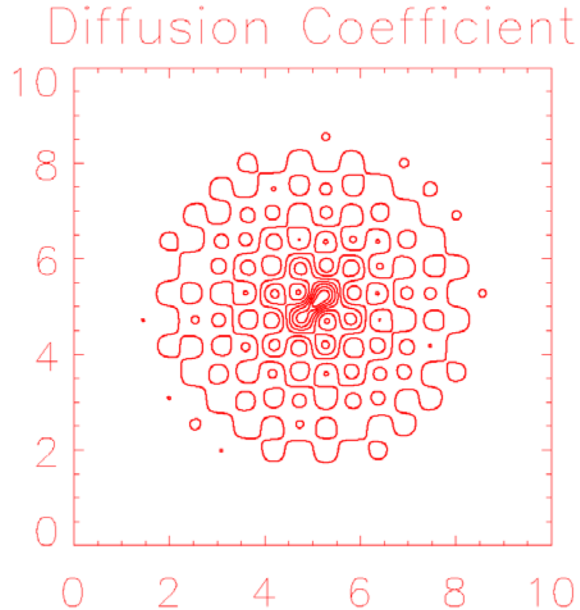

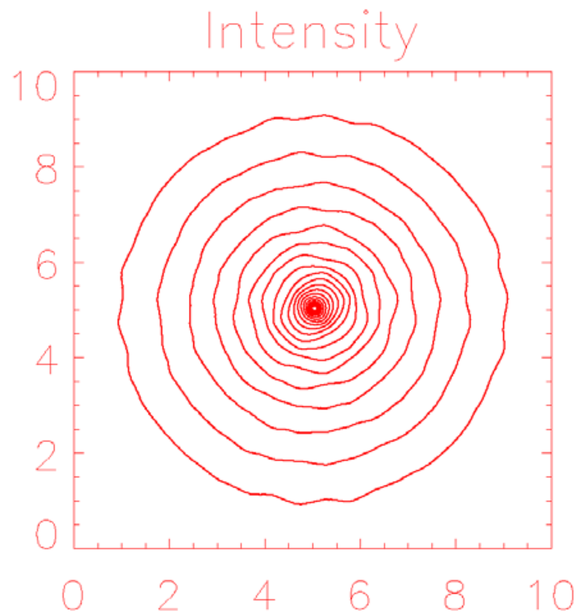

Note that the spatial gradient changes sign.

This sign change in the gradient does not happen in a one-D model.

So perhaps we need not be near the center, just at a local minimum in the anisotropy.

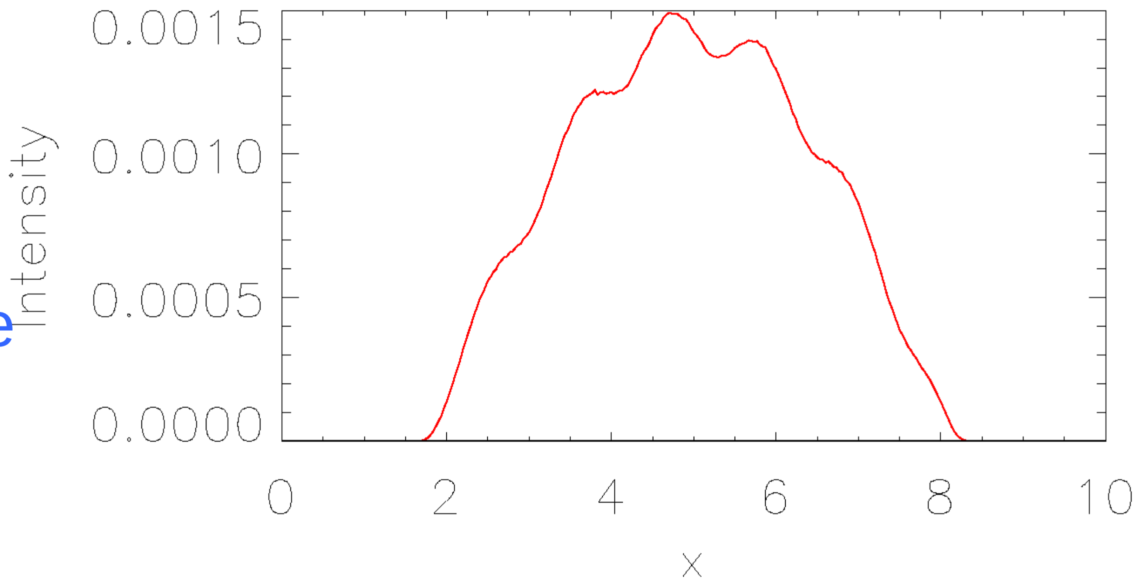

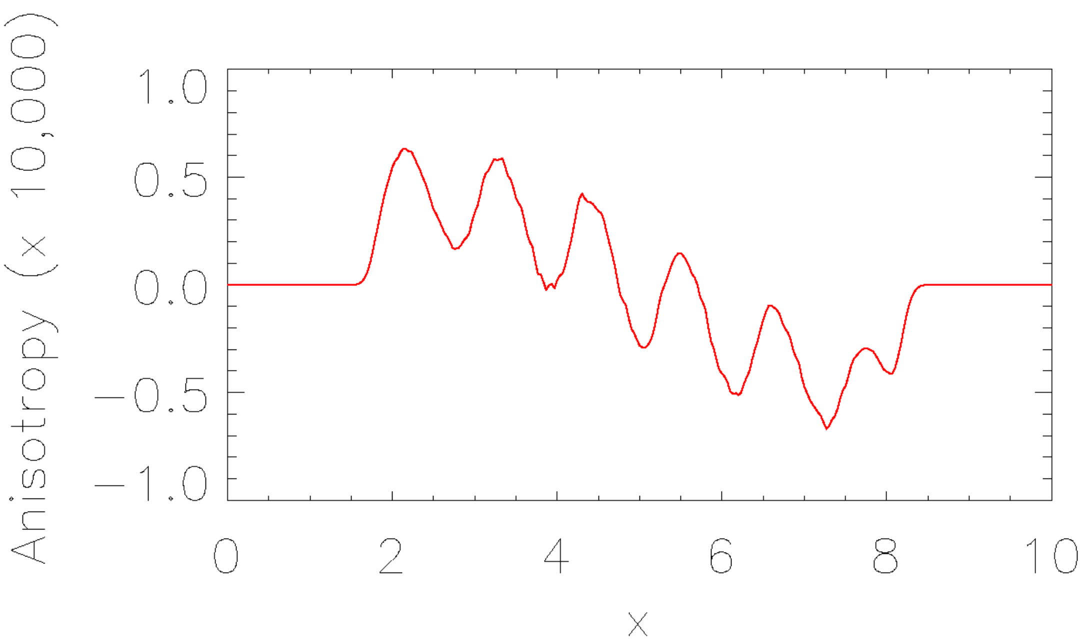

Even more-complicated scenarios are possible.

Results of a model calculation with multiple sources, as in Strong and Moskalenko..

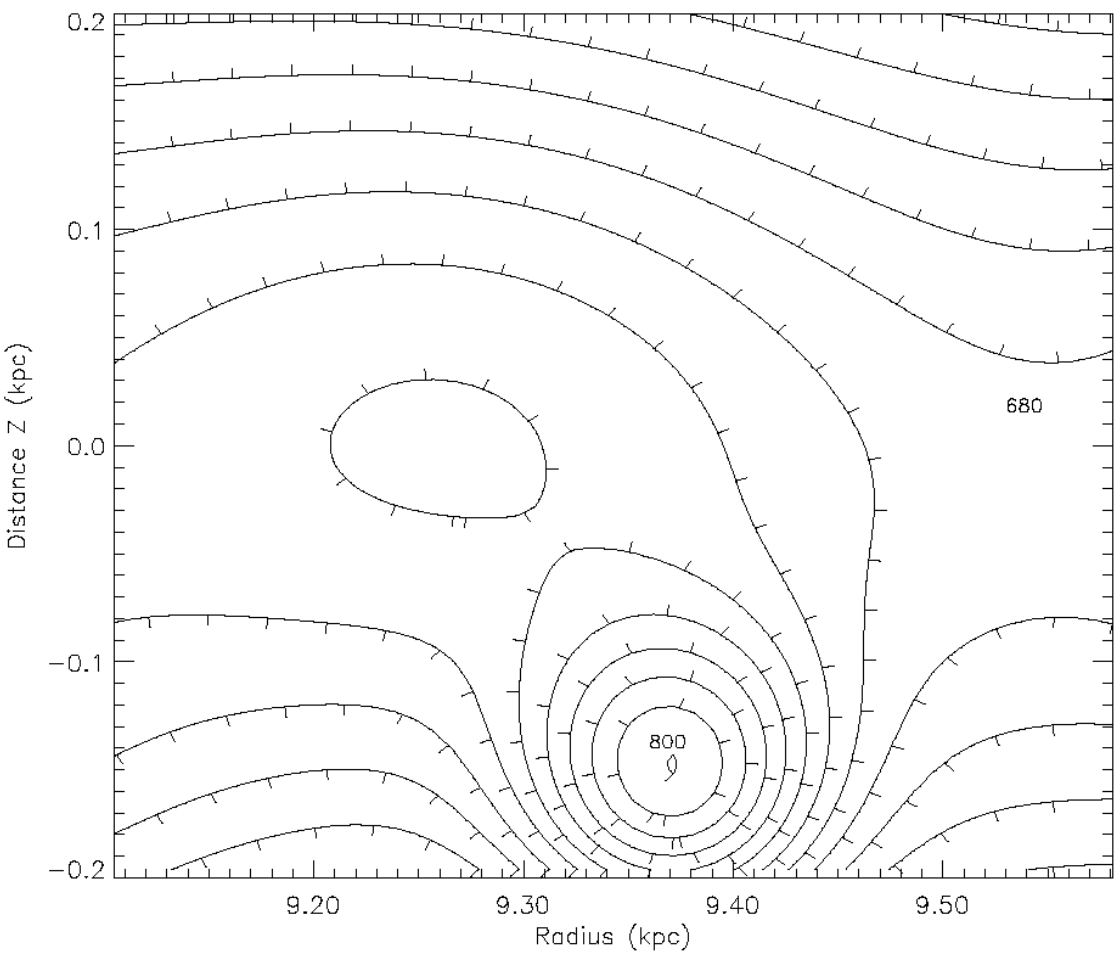

Conclusions

- The observed anisotropies of cosmic rays at both small scales and large scales may be a direct result of interstellar turbulence.
- Simple considerations suggest that some puzzling effects might be explained in terms of turbulent fluctuations at both large and small scales. Perhaps other anomalies, such as energ spectra, etc, may also be a consequence of local interstellar turbulence.
- Are there observational tests for these ideas?

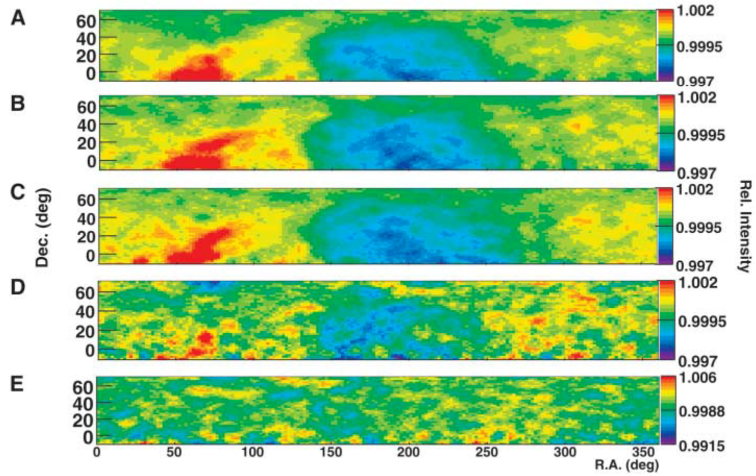

Fig. 3. Celestial CR intensity map for different representative CR energies. (**A**) 4 TeV; (**B**) 6.2 TeV; (**C**) 12 TeV; (**D**) 50 TeV; (**E**) 300 TeV. Data were gathered from 1997 to 2005. The vertical color bin width is 2.5×10^{-4} in [(A) to (D)] and 7.25×10^{-4} in (E) for different statistics, all for the relative CR intensity.

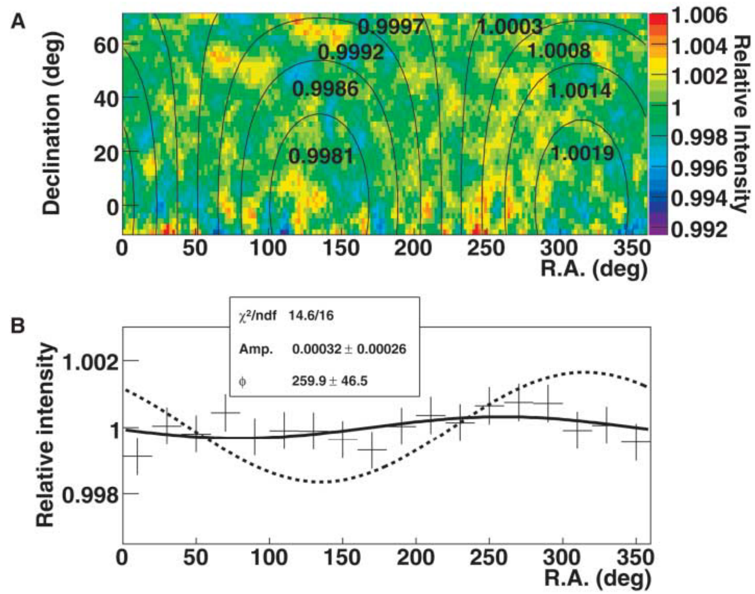

Fig. 4. Celestial or 2D local sidereal time CR intensity map and its 1D projection in the R.A. direction for 300 TeV CRs of all data. (**A**) The colored map is the same as Fig. 3E. The contours are the "apparent" 2D anisotropy expected from the Galactic CG effect. The width of the vertical color bin is 7.25×10^{-4} for the relative intensity in (A). The 1D projection is in map (**B**) for Dec between 25° and 70°, where the dashed line is the expected Galactic CG response and the solid line is the best fit to this observation using a first-order harmonic function. The fitting function is in the form of Amp $\times$ cos(R.A. $-$ ϕ) where ϕ is in degrees and Amp is the amplitude. The χ^2 fit involves the ndf given by the number of bins minus two for the two fitting parameters Amp and ϕ. The data shows no Galactic CG effect with a confidence level of ~5 SD.

At TeV energies. δ, relative to the local interstellar medium is $< \approx 3 \times 10^{-4}$

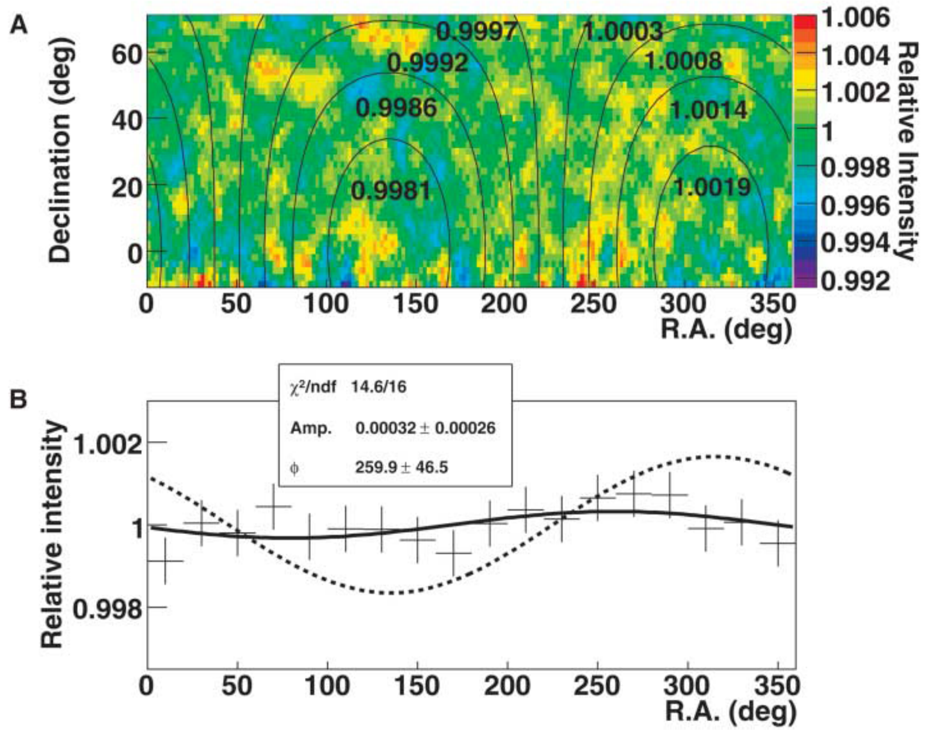

Fig. 4. Celestial or 2D local sidereal time CR intensity map and its 1D projection in the R.A. direction for 300 TeV CRs of all data. (**A**) The colored map is the same as Fig. 3E. The contours are the "apparent" 2D anisotropy expected from the Galactic CG effect. The width of the vertical color bin is 7.25×10^{-4} for the relative intensity in (A). The 1D projection is in map (**B**) for Dec between 25° and 70°, where the dashed line is the expected Galactic CG response and the solid line is the best fit to this observation using a first-order harmonic function. The fitting function is in the form of Amp $\times$ cos(R.A. $-$ ϕ) where ϕ is in degrees and Amp is the amplitude. The χ^2 fit involves the ndf given by the number of bins minus two for the two fitting parameters Amp and ϕ. The data shows no Galactic CG effect with a confidence level of $\sim$5 SD.

From Amenomori, et al, Science, 2006

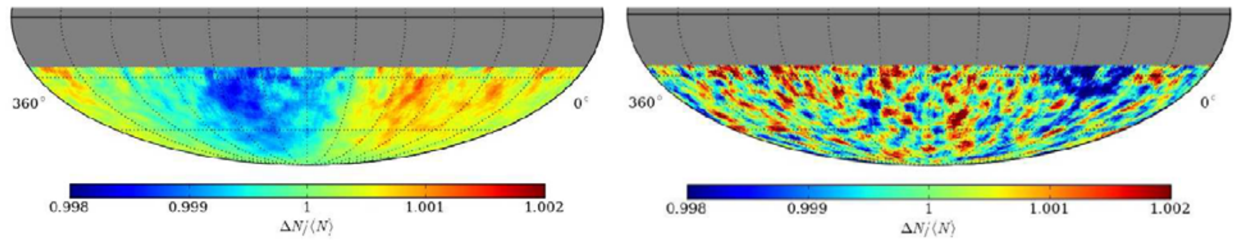

Figure 1: Relative intensity $\Delta N/\langle N\rangle$ of the IC59 data in equatorial coordinates for the 20 TeV (*left*) and the 400 TeV (*right*) energy sample. The sky maps are smoothed within 3° to match the angular resolution of the data.

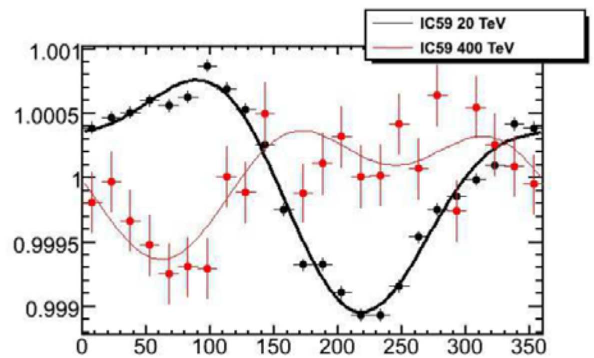

Figure 2: One-dimensional projection in right ascension α of the 20 TeV (black) and 400 TeV (red) maps in Fig. 1. The data are shown with statistical uncertainties, and the lines correspond to the first and second harmonic fit.